Cement and Concrete Research 41 (2011) 422–428

Contents lists available at ScienceDirect

Cement and Concrete Research

journal homepage: http://ees.elsevier.com/CEMCON/default.asp

Impact of the alkali–silica reaction products on slow dynamics behavior of concrete

Apedovi S. Kodjo [a,*], Patrice Rivard [a], Frederic Cohen-Tenoudji [b,c], Jean-Louis Gallias [d]

[a] Groupe de recherche en Auscultation et Instrumentation (GRAI), Civil Engineering Department, Université de Sherbrooke, Canada J1K 2R1
[b] UPMC Univ. Paris 06, UMR 7190, Institut Jean le Rond d'Alembert, F-75005 Paris, France
[c] CNRS, UMR 7190, Institut Jean le Rond d'Alembert, F-75005 Paris, France
[d] Laboratoire de Mécanique Matériaux du Génie Civil (L2MGC), Université de Cergy-Pontoise, Neuville-sur-Oise, 95031 Cergy Pontoise Cedex, France

ARTICLE INFO

Article history:
Received 6 September 2010
Accepted 12 January 2011

Keywords:
Crack detection (B)
Alkali–silica reaction (C)
Characterization (B)
Mechanical properties (C)
Nonlinear acoustics

ABSTRACT

Several nondestructive techniques based on acoustics are frequently used to assess the condition of engineering materials. It has been demonstrated that nonlinear acoustics is more sensitive for detecting micro-cracks. The main challenge, regarding the assessment of alkali–silica reaction (ASR) damage in concrete, remains in the efficiency of the technique to distinguish ASR from other damaging process. Based on the fact that ASR produces a swelling viscous gel, a new approach developed for finding a signature to ASR is investigated in this paper. The research was focused upon the specific behavior of ASR causing the presence of viscous gels in micro-cracks and porosity compared with mechanical damage where cracks are empty. With this approach, the concrete response to slow dynamics tests was analyzed. The Burger spring–damping model was used for interpreting the results. This research showed that the slow dynamics technique presented here can detect cracking in concrete and that the time response to an external excitation of concrete damaged by ASR is different from that of concrete mechanically damaged.

1. Introduction

Alkali–silica reaction (ASR) causes the expansion and cracking of numerous concrete structures worldwide. The expansion is due to the formation of continuing chemical reaction products, the silica gels, which swell at moisture levels above about 85% R.H. These expansive gels create internal stresses and lead to the formation of a micro-crack network through the concrete when the material tensile strength is reached. Moreover, gels have a viscous behavior; under external and internal stresses, they slowly move in porous space and cracks and enhance the hysteretic behavior of concrete. The viscous property of gel is conserved over time even if partial crystallization occurs with ageing [1,2]. The hysteretic behavior can be observed from successive static loading cycles applied to ASR-affected concrete [3].

Assessment of concrete damage is an important issue and many nondestructive methods based on nonlinear acoustics have been proposed to evaluate it [4–9]. They have been validated in heterogeneous materials such as rocks and concrete and appeared to be very sensitive to micro-cracks induced by mechanical or thermal damage, for instance. Recently, Chen et al. have applied nonlinear acoustics to evaluate damage due to ASR in mortar samples [10,11]. They showed that the techniques of nonlinear resonance and modulation frequency allowed detecting the formation of micro-cracks in the initial phase of ASR in ultra-accelerated expansion tests. However, this approach seemed to be inefficient to specify if ASR-induced damage has a particular signature comparatively to other causes of damage (mechanical, thermal, etc.)

The aim of this paper is to identify the effects of expansive viscous gels associated with ASR on the nonlinear behavior of concrete, focusing on their specific action, when compared with mechanical damage. The presence or absence of gels in porous space and micro-cracks has an effect upon the concrete response to slow dynamics tests performed during conditioning phase where the samples are driven at large excitation amplitude for several minutes. This dynamic approach could be compared to a conventional static creep test where the material deformation submitted to constant load is analyzed with regards to time.

In all papers published on this topic, the relaxation phase has been mostly used to study the slow dynamic behavior of materials. The conditioning phase is of little interest since the response of micro-cracks during conditioning is almost instantaneous: the cracks are often empty. An approach based on creep phenomenon is presented in this paper in an attempt to detect the presence or absence of reaction products in the cracks. Nonlinear techniques are based on opening/closing of micro-cracks under high acoustic pressures. The high acoustic waves propagate through the material and cause the opening and/or closing of the micro-cracks and the inter-grain contacts. Thus, the high acoustic stress generated by the nonlinear resonance technique allowed performing a creep test directly on the micro-cracks. The assumption is then intuitively made that empty cracks will show creep behavior close to perfect elastic material and cracks fill with reaction products will show behavior close to viscous

* Corresponding author at: Civil Engineering Department, Université de Sherbrooke, J1K 2R1 Canada. Tel.: +1 819 821 8000x65681; fax: +1 819 821 7974.
E-mail address: Apedovi.kodjo@usherbrooke.ca (A.S. Kodjo).

0008-8846/$ – see front matter © 2011 Elsevier Ltd. All rights reserved.
doi:10.1016/j.cemconres.2011.01.011

material. The time response of creep is expected to be indicative of the presence or absence of reaction products within the cracks.

2. Theoretical background

Nonlinear acoustics consists in applying high amplitude stress waves on material, which introduce "significant local deformations". These deformations cause the modification of the material elastic coefficients, inducing a nonlinear behavior. The cause of the nonlinearity in concrete is related to the micro-defects within the concrete. The micro-cracks are subjected by the propagating compression waves to various closing/opening cycles due to the oscillating high pressure. The nature of these cycles is also dependant of the crack orientation with respect to the applied local stress. Depending on this orientation, the material rigidity will either be reduced when the stress load is parallel to the crack (crack is opened) or be increased when the stress load is perpendicular to the crack (crack is closed) [12].

This nonlinear behavior is highlighted by numerous indicators, such as resonant frequency shift, discrete memory, nonlinear wave interaction, harmonic generation, nonlinear attenuation, fast and slow dynamics response [4,13–17]. Many techniques have been developed for characterizing the nonlinear effects in materials; quasi-static test [18], phase comparison method [19] finite amplitude method [20], modulation method [4,8], and resonance bar test [4,8]. Among these experimental approaches, the resonance bar technique has been, so far, the most popular technique for investigating nonlinear effects such as the resonant frequency shift, the nonlinear attenuation, and the slow dynamics.

To describe nonlinear behavior, such as nonlinear hysteresis, the model of Preisach and Mayergosz (P–M) has been used as the basis in the development of some nonlinear models [4,21–24]. The P–M model is based upon the assumption that the macroscopic elastic properties of the tested material stem from the integral response of a large number of individual elastic elements (grain contact, micro-cracks and other discontinuities). This model takes into account the nonlinear hysteresis according to the following stress–strain relationship: [8,24]:

$$\sigma = \int M\left(\varepsilon, \frac{\partial \varepsilon}{\partial t}\right) d\varepsilon \tag{1}$$

Where σ is the stress, ε is the strain and the function M is the nonlinear and hysteretic mechanical modulus given by:

$$M\left(\varepsilon, \frac{\partial \varepsilon}{\partial t}\right) = M_0\left[1-\beta\varepsilon-\delta\varepsilon^2-\alpha\left(\Delta\varepsilon + \varepsilon(t) sign\left(\frac{\partial \varepsilon}{\partial t}\right)\right)\right] \tag{2}$$

Where M_0 is the linear modulus, β and δ represent classical nonlinear parameter and α is the hysteretic nonlinearity parameter that quantifies the nonlinear hysteresis, which is the principal phenomenon prevailing in porous material such as concrete [4,8,12,23,24]. $\Delta\varepsilon$ is the strain amplitude, $\varepsilon(t)$ is the instantaneous strain as a function of time, $sign\left(\frac{\partial \varepsilon}{\partial t}\right) = 1$ for $\frac{\partial \varepsilon}{\partial t} > 0$(loading) and $sign\left(\frac{\partial \varepsilon}{\partial t}\right) = -1$ for $\frac{\partial \varepsilon}{\partial t} < 0$ (unloading).

This function shows that the modulus depends not only on the current stress state, but also on the orientation of the strain tensor and the loading history of the material.

Previous researchers have reported that the nonlinear hysteresis can be characterized by the slow dynamics effect [4,6,9]. Slow dynamics refers to the temporary alteration (decrease) of the material average modulus of elasticity during excitation. After wave excitation, it takes some time for the material modulus to recover its original state. So, a slow dynamics test has basically two phases: 1) a conditioning phase during which the material is subjected to high excitation amplitude and 2) a relaxation phase during which high excitation is turned off and low excitation amplitude is used to track the material response [21]. Almost all the previous researches have been focused on the relaxation phase. A few references exist on the conditioning phase indicating that the process of conditioning and recovery is not symmetric; the conditioning phase occurs quickly, whereas the recovery shows a different behavior [14,15].

Based on a phenomenological description, several researchers proposed [4,13];

$$\tau_r \frac{d\Delta M}{dt} + \Delta M = \lambda G \tag{3}$$

Applying an excitation having the form $G\theta(t)$ onto a material governed by Eq. (3), where $\theta(t)$is the Heaviside function defined by $\theta(t) = 0$ for $t<0$, $\theta(t) = 1$for $t \geq 0$, G is the modulus amplitude when t tends to infinity, λ is an hysteresis coefficient and τ_r the relaxation time, the specimen response form is given by:

$$\Delta M(t) = \lambda G\left(1-e^{-t/\tau_r}\right) \tag{4}$$

All experiments conducted on rock samples showed that the relaxation process was logarithmic in time rather than exponential [4,14]. In fact, the simple model proposed in Eq. (4) for the nonlinear portion of the elastic modulus, assumes a constant relaxation time (or sometimes several time constants) [4,13]. With the attempt to simplify the analysis of the mechanical behavior of the elements influencing the material response, simple models such as described in Eq. (4) are generally used, even though the real process does not behave so simply.

In this paper, in order to study the viscoelastic behavior of ASR-damaged material (cracks filled with viscous gels), the conditioning phase will be used like a conventional creep test and the physics of the behavior will be analyzed by the simple mechanical models often used to predict a viscoelastic behavior of material. It is well-known that in materials submitted to static stress during the time (t_1-t_0), the elastic elements instantly deform. In the case of a material containing micro-cracks, this deformation can be explained by the elastic opening of micro-cracks) (Fig. 1a). On the other hand, fully viscous elements show a linear strain variation with time (Fig. 1b). For

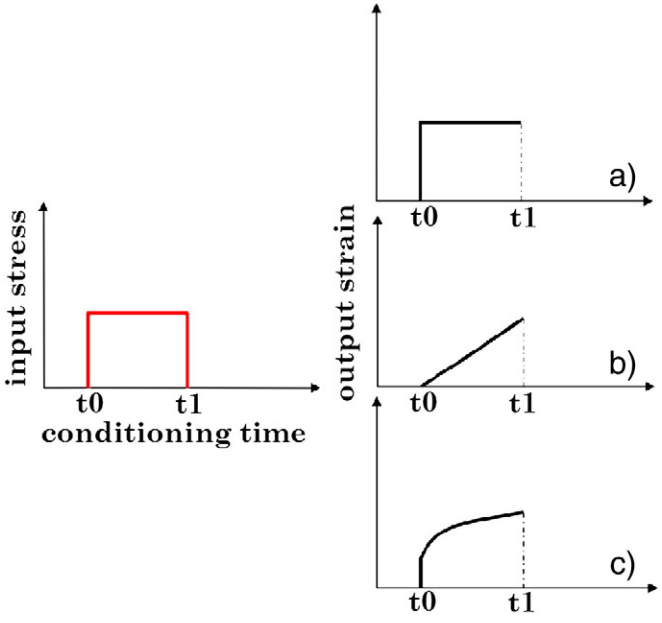

Fig. 1. Schematic material creep behavior a) elastic material, b) fully viscous material, c) viscoelastic material.

viscoelastic elements, the strain evolution is between the two previous cases, following a stretched exponential shape (Fig. 1c).

Considering that the micro-cracks filled with gels (depicted as elongated ellipses in Fig. 2a) present a viscoelastic behavior, the response during conditioning (when material is disturbed at high amplitude stresses) can be modeled according to the four-element model, called Burger model (Fig. 2b). It is a combination of the Maxwell element and Kelvin element in series [25–27]. It is the simplest model exhibiting all the essential features of viscoelasticity, and it has been widely used to model the creep behavior [28].

During conditioning, a given crack is subjected to stress in the direction j (stress coming from high acoustic amplitude applied upon the material), and expands in the perpendicular direction i causing its opening. In the direction i, it may be considered that negative stress σ_i (expansion stress) leads to a deformation $\varepsilon_i(t)$. The Burger model states that, when a constant load is applied, the total deformations of the three terms in the model (composed of a single spring with elastic coefficient E_1, the dashpot with viscosity η_1 and the spring with elastic coefficient E_2 parallel to the dashpot with viscosity η_2) can be expressed as [26,28]:

$$\varepsilon_i(t-t0) = \frac{\sigma_{i0}}{E_1} + \frac{\sigma_{i0}}{\eta_1}(t-t_0) + \frac{\sigma_{i0}}{E_2}\left[1-e^{-\frac{E_2}{\eta_2}(t-t_0)}\right] \quad (5)$$

Where σ_{i0} represents the negative constant stress in the direction i (expansion), t_0 the initial time whilst the constant stress is applied, and t the time.

Eq. (5) expresses both the evolution of the crack deformation in the direction i and the opening of the cracks. That deformation was referred previously as "significant local deformation". The variation of the deformation will induce a local variation of the viscoelastic behavior of the material under the same behavior law:

$$\Delta M(t-t_0) = G_1 + G_2\left[1-e^{-\frac{(t-t_0)}{\tau}}\right] + \frac{1}{T}G_3(t-t_0) \quad (6)$$

where ΔM is the variation of the modulus of the material, T the conditioning duration, G_1,G_2,G_3 are defined by the variation $\Delta M(0)$ at the initial moment (t_0) when the stress is applied: $\Delta M(0) = G_1$ and the variation of modulus at the end of the conditioning time T: $\Delta M(T) = G_1 + G_2 + G_3$ considering T to be sufficiently long.

Eq. (6) represents the behavior of the material during conditioning. This equation is similar to Eq. (3), which illustrates the dynamic behavior of the material during the slow relaxation phase.

However, like for the relaxation experimental curves, the conditioning experimental curves have a logarithmic shape. Even if the Burger mechanical model presented in Eqs. (5) and (6) facilitates the visualization and the physical analysis of deformations in the creep test, it does not describe accurately the reality seen through the experimental curves. This can be explained by the fact that the materials (in our case micro-cracks) cannot be represented by a few springs and dashpots only. In fact, the response time of the material results from the full response time of each element and unfortunately, improving quantitative accuracy by using generalized model with many elements could increase mathematical complexity to the point where the number of parameters may be too large to handle [29]. To avoid the complexity of the model and approximate experimental data with accuracy, some authors use Weibull distribution function and Kohlrausch–Williams–Watts (KWW) stretched exponential function [30,31]. It was found that creep behavior could be accurately represented by these functions [30]. In order to extract the creep response time $\tau$from the experimental data, we use a mathematical fit model based on the Weibull distribution function and KWW stretched exponential function. This model allowed the adjustment of the curve shape to best fit with the experimental curve. The model is defined by the following equation:

$$\Delta M = G_1' + G_2' e^{-\left(\frac{t-t_0}{\tau}\right)^{\gamma}} \quad (7)$$

where G_1' and G_2' depend on the initial and final conditions of the modulus amplitude, τ is the "average" response time during conditioning, and γ is an exponent factor used to adjust the shape of the conditioning curve. It should be noted that parameter γ has not been given a physical description, but with γ between 0 and 1, the graph $\Delta M(t)$ best fits with the response that is experimentally observed.

3. Materials and experiments

Tests were conducted on two concrete cores drilled from a large hydraulic civil engineering structure located in Eastern Canada suffering from ASR and on two nonreactive laboratory concrete samples that have been damaged by compressive load. All specimens are cylindrical with dimensions ($\phi 100 \times 200$ mm). Table 1 presents the properties of the investigated samples after damaging. Despite the fact that the dimension of larger aggregate (about 50 mm) in the core is close to the specimen dimension, the influence of the aggregate size

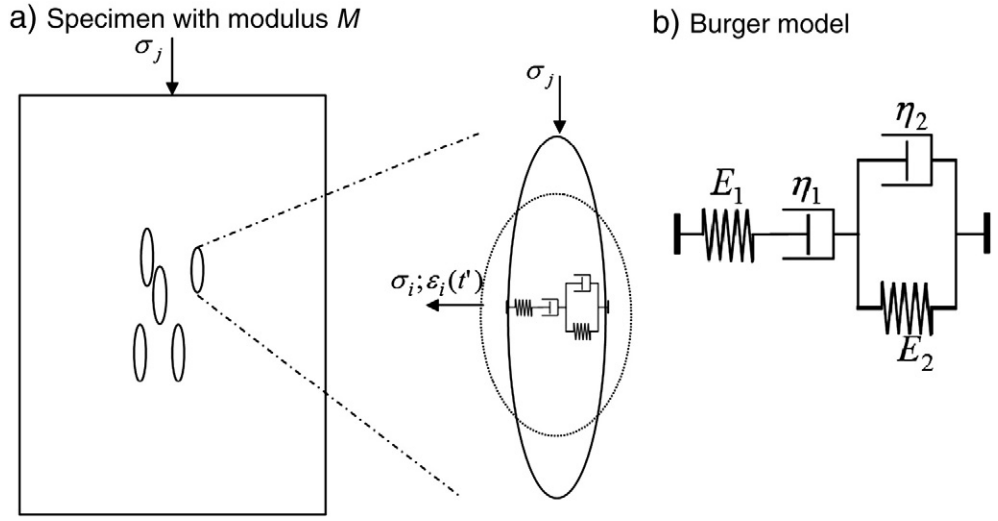

Fig. 2. Generic viscous-elastic model of cracks in one dimension using Burger model. a) Specimen with modulus. b) Burger model.

Table 1
Properties of investigated samples.

	E1	E2	E3	E4
Type of damage	Mechanical	Mechanical	ASR	ASR
Compressive strength	80 MPa	58 MPa	27 MPa	32 MPa
Dynamic Young modulus	N/A	N/A	23.7 GPa	24.5 GPa
Static Young modulus	38 GPa	44 GPa	N/A	N/A
Ultrasonic pulse velocity	3905 m/s	4667 m/s	3560 m/s	3580 m/s

is negligible compared with the ASR effect. That has been previously verified in the lab on ASR-damaged concrete made with small aggregate.

The structure of 15 m in height was built nearly 50 years ago and is affected by ASR, detected approximately 20 years after its construction. Several recurring operating problems have been reported over the last years. Total vertical displacement rates related to the expansion of concrete vary between 0.1 mm/year and 1.6 mm/year. The ASR in this structure is due to the use of a reactive crushed siliceous limestone as coarse aggregate in the concrete [32]. Fig. 3a shows the presence of reaction products filling cracks and porosity.

The mechanical damage was obtained by applying a uniaxial stress of about 90% of the compressive strength to create micro-cracks. Fig. 3b shows the crack network. Table 1 summarizes the main properties of the investigated samples.

The concrete cylinder is excited with a pure sine wave. For a specific voltage, a frequency sweep was performed to find the specimen resonant frequency. The signal is produced by a low frequency generator Agilent 33250A. The signal is amplified in order to drive the piezoelectric actuator that excites one end of the specimen. At the other end, an ICP accelerometer detects the signal after its propagation through the specimen. The signal detected by the accelerometer is conditioned before being converted to digital signal by the computer (Fig. 4).

To obtain the slow dynamics response, the sample is driven according to the following protocol: the voltage of the actuator is initially set to obtain a strain of 1.7 10^{-5} mm; the specimen at that time has a resonant frequency of f_0. The voltage is then quickly increased to obtain a strain of 40 10^{-5} mm during 5000 s which represents the conditioning phase, and then decreased back to a strain of 1.7 10^{-5} mm during 5000 s (the relaxation phase). The analysis was carried out during the conditioning phase.

The specimen was assumed to be sufficiently long compared with its diameter in order to assume a Young extensional resonant mode for a free rod. In this mode, the wave velocity is $c = 2lf = \sqrt{\frac{M}{\rho}}$, where l is the length of the specimen, f the resonant frequency, M the dynamic modulus of elasticity (Young modulus) and ρ the density of the specimen. Therefore, ΔM can be considered to be proportional to the variation of the square of the resonant frequency, Δf^2. From the variation of the square of the resonant frequency, the relative variation of the dynamic modulus can be estimated as: $\frac{\Delta M}{M_0} = \frac{\Delta f^2}{f_0^2}$.

4. Results and discussion

Fig. 5 shows the resonance curve when the specimen is excited with low stress: the resonance frequency of the mechanically damaged sample is about 4950 Hz and about 8670 Hz for the ASR-damaged sample. During the transition of the excitation drive from low to high values, an instantaneous decrease is observed in the material resonant frequency: the frequency decreases from 4950 Hz to 4674 Hz for the mechanical damage and from 8670 Hz to 8626 Hz for the ASR damage (Fig. 6). This behavior stems from fast dynamics effect, which can be explained by the opening of micro-cracks, reducing the stiffness of the material and shifting its resonant frequency toward lower values.

During the conditioning phase, when high excitation stress is maintained on material during about 5000 s, the material's dynamic modulus continues to change. In fact, the resonant frequency decreases again by about 0.79% (from 4674 Hz to 4637 Hz) for specimen E1 (mechanically damaged) and about 0.30% (from 8626 Hz to 8600 Hz) for specimen E3 (ASR damaged), from its value at the beginning of high amplitude excitation (Fig. 6). This is the slow dynamics effect, where the material rigidity gradually shifts towards an equilibrium state under high excitation stresses. At the microscopic scale, it means that micro-cracks gradually open up to their maximum opening state.

For practical reasons, to analyze and quantify the time taken by the material to reach the equilibrium state under high stress, the 5000 s conditioning time was considered as infinite. Note that this is obviously not the case, especially for the specimens damaged by ASR. Fig. 7 shows that the response time τ during the conditioning is longer for the concrete damaged by ASR. Indeed, the expression $\tau = \frac{\eta}{M}$ means that the creep response time τ is proportional to the viscosity η brought by ASR products. The model described in Eq. (7) was used after adjusting the parameter γ to 0.7 in order to fit the experimental curves. The value of γ was kept to 0.7 for all specimens, while the value of τ was adjusted each time to fit the model to the experimental curve. From the relative variation of the square of the specimen resonant frequency, the creep time was extracted and found to be equal to 1400 s for specimens E3 and E4 that were damaged by ASR, while it was 400 s for E1 and E2 mechanically damaged samples (Fig. 8). This longer creep time can be explained by the damping of the

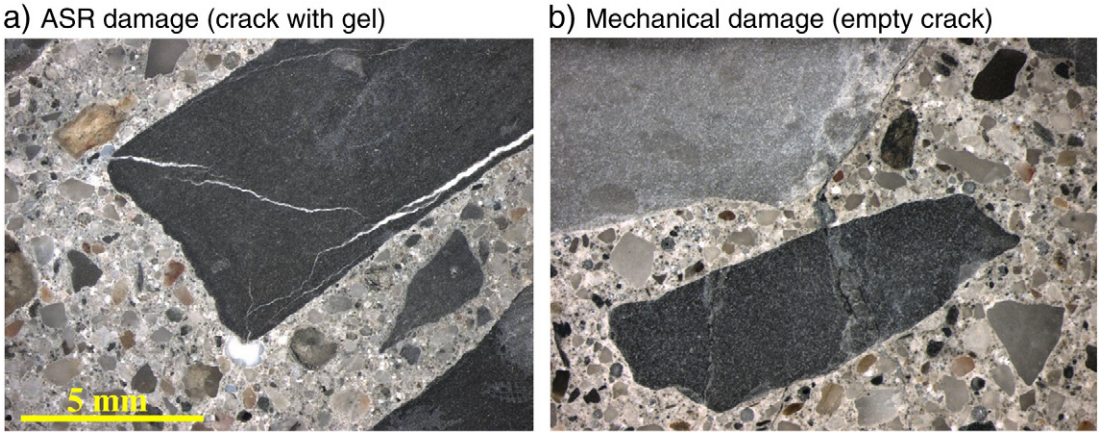

Fig. 3. Polished section of investigated concrete sample. a) ASR damage (crack with gel). b) Mechanical damage (empty crack).

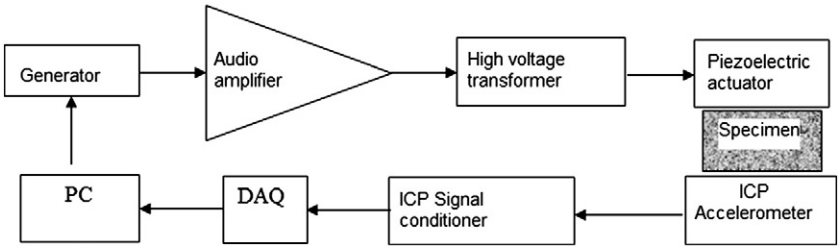

Fig. 4. Typical resonance bar experiment.

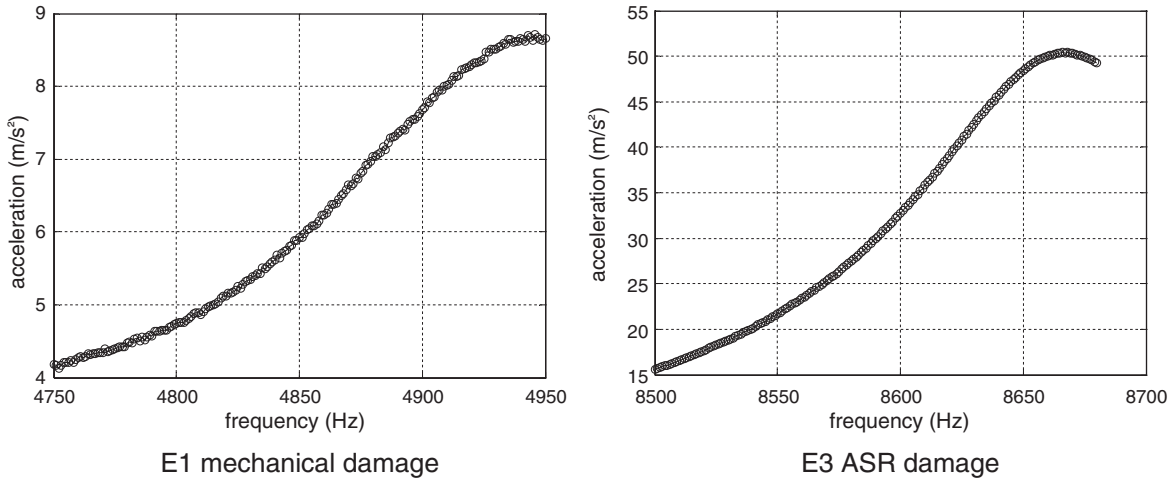

Fig. 5. Resonance curve before the conditioning of concrete specimens. E1 mechanical damage. E3 ASR damage.

high stress during propagation caused by the presence of ASR products, and the change of the micro-cracks (filled with gel) properties during the conditioning.

Remember that in an attempt to model the nonlinear behavior according to the Preisach and Mayergoz hypothesis, two pressures (open and closed pressures) are associated with each UHM [4,7,22] (each micro-crack in our case).

Thus, all cracks for which the opening pressure is less than the applied pressure should open [4,7,22]. The addition of a viscosity effect involves that the opening pressures change according to the duration of the applied pressure. Suppose a crack having an opening pressure of P1 without viscosity and P2 with viscosity. A viscous crack (filled with gel) subjected to a pressure P as P1<P<P2, will not open immediately. The pressure being kept, the opening pressure P2 will drop with time and become lower than the applied pressure, leading to its opening. This explains the slow creep behavior that was observed. Without viscosity, cracks opens as soon as the opening pressure is reached, whatever the size of crack, leading to a quick response to the applied pressure. The possibility that the observed creep effects are due to the large cracks (without viscosity) can be

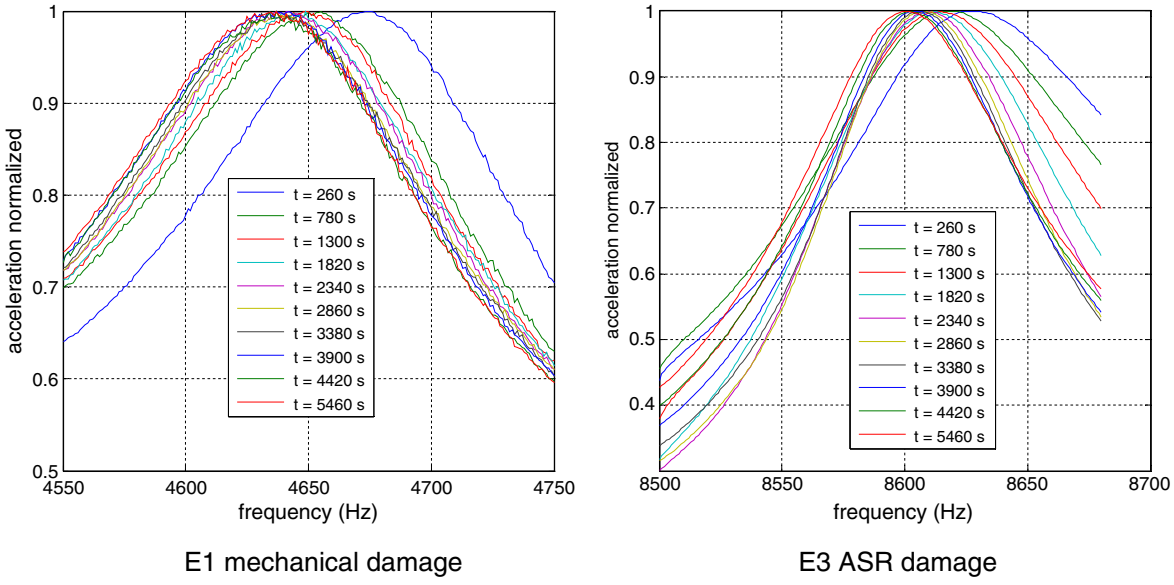

Fig. 6. Variation of resonant frequency during the conditioning of concrete specimens. E1 mechanical damage. E3 ASR damage.

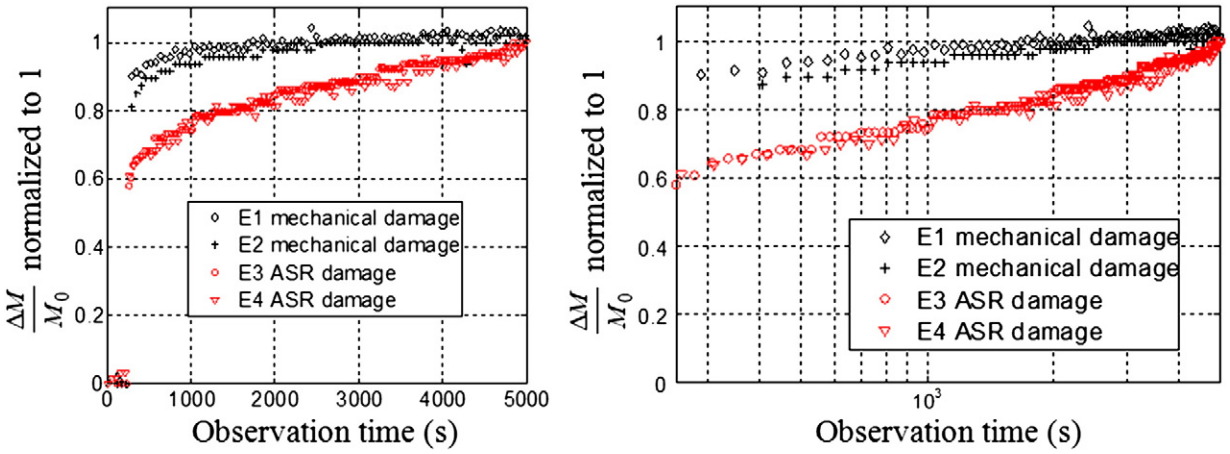

Fig. 7. Relative variation of square of resonant frequency during conditioning. The logarithmic time scale plot reveals that creep response has logarithmic time behavior.

eliminated if we consider that the crack behavior is complying with the Preisach and Mayergoz hypothesis, which does not consider the viscous effect.

Tests have been conducted on samples of various sizes and exhibiting different damage levels and results showed that only the amplitude of the instantaneous relative variation of the resonant frequency was sensitive to the damage level. The response time to creep was not affected [7]. Therefore, the relative variation of the resonant frequency was normalized to 1 for a duration considered as long enough (5000 s) in order to highlight the creep time response. It must be recalled that the final model used to fit the curve for evaluating the creep delay is a mathematical model that does not have any physical consideration. The physical model used in the theoretically background section to explain the physics of the phenomenon is

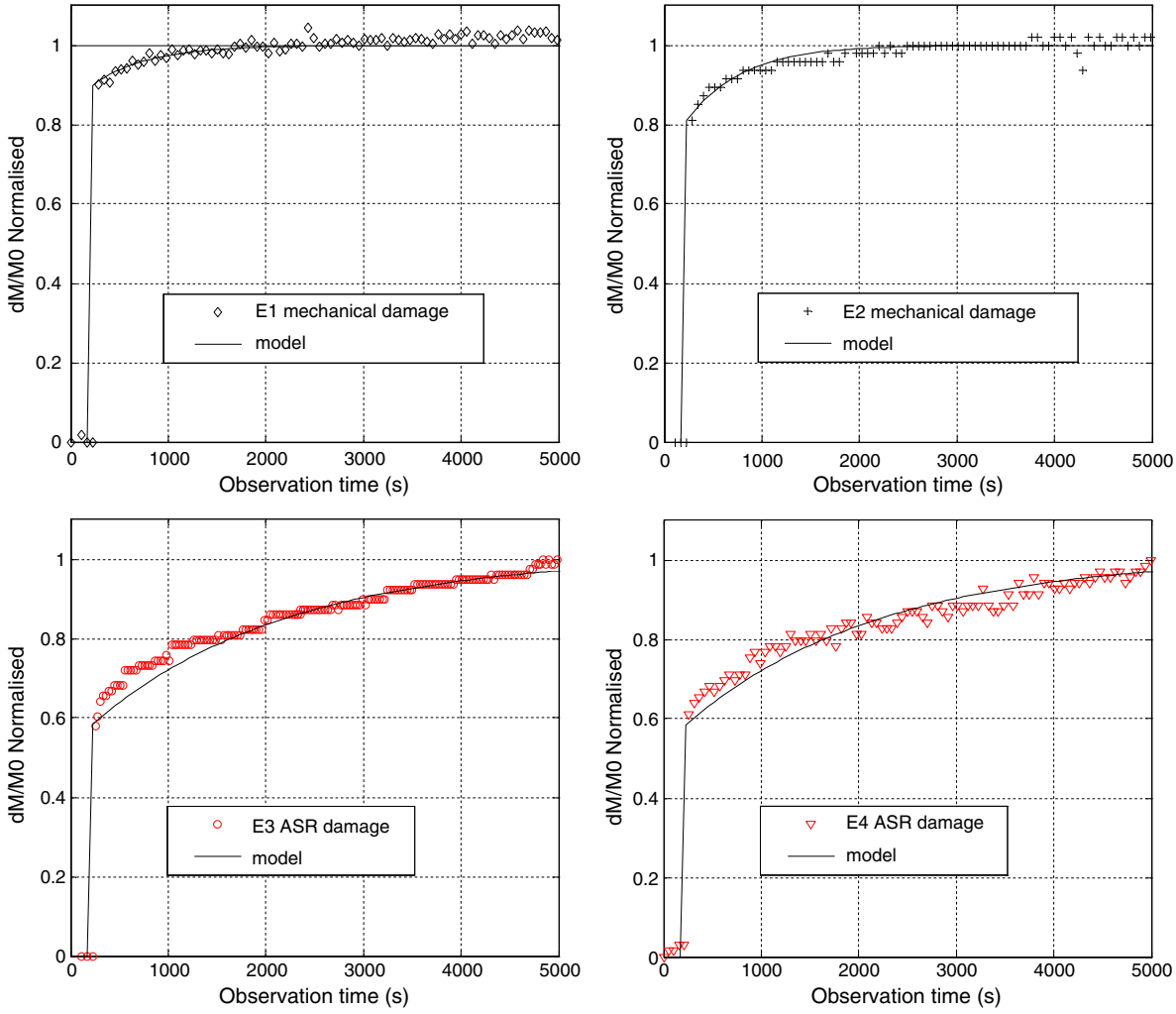

Fig. 8. Relative variation of square of resonant frequency during conditioning. Each curve is fit by the model in Eq. (7) in order to extract the creep time.

a model of one hysteretic element that can be one crack filled or not with gel, or one micro-defect, or even an inter-grain contact. Thus, the global response of the material is the sum of the response of all the hysteretic elements. At the current stage of our research, we could not find a simple physical model describing the global creep behavior of the material taking into account each hysteretic element behavior.

5. Conclusion

The results presented here show that it is possible to perform creep test from nonlinear acoustic measurements, following slow dynamics concepts. The conditioning phase of the slow dynamics test which involves subjecting the material to an excitation of high acoustic stress for a relatively long duration was used. The creep response time of the material was examined during this test through the relative variation of the square of the resonant frequency of the samples; this resonant frequency square is directly proportional to the variation of the dynamic modulus of the material. The conditioning test allows revealing that the cracks taking place in creep process have either viscous or elastic behavior. These tests confirm our hypothesis that intuitively attributed a viscous behavior to the ASR reaction products. In fact, these tests show that the samples with the reaction products have a creep response time longer than those with empty cracks (with a ratio of more than 3). Thus, this technique highlights the presence or absence of reaction products of ASR. It allowed differentiation of this type of damage compared with mechanical damage. One objective of this research is to quantify the degree of the ASR damage using nonlinear acoustics technique. It was found that nonlinear parameter alpha and beta increased with ASR damage [7]. It was also found that the beginning of the conditioning test (when the transition of the excitation drives from low to high values) led to an instantaneous relative variation of the square of the resonant frequency, which was proportional to the level of ASR damage [7,33]. Further work is underway in an attempt to find a relationship between the instantaneous relative frequency variation and one of the nonlinear parameter. That will allow this technique highlighting not only the ASR damage but also the damage level in the concrete.

Acknowledgements

Financial support has been provided by the Natural Science and Engineering Research Council of Canada (NSERC) and by the Fonds Québécois de Recherche sur la Nature et les Technologies (FQRNT).

References

[1] F. Noronha Fernandes, M. Teles, Examination of the concrete from an old Portuguese dam: texture and composition of alkali–silica gel, Materials Characterization 58 (2007) 1160–1170.
[2] F. Noronha Fernandes, M. Teles, Microscopic analysis of alkali-aggregate reaction products in a 50-year-old concrete, Materials Characterization 53 (2004) 295–306.
[3] N. Smaoui, M.A. Bérubé, B. Fournier, B. Bissonnette, B. Durand, Evaluation of the expansion attained to date by concrete affected by alkali–silica reaction. Part I: experimental study, Canadian Journal of Civil Engineering 31 (2004) 826–845.
[4] L.A. Ostrovsky, P.A. Johnson, Dynamic nonlinear elasticity in geomaterials, Bologna, Società Italiana di Fisica, Collection La Rivista del Nuovo Cimento 24, 2001,, 46 pp.
[5] X.J. Chen, J.H. Kim, K.E. Kurtis, J. QU, C.W. Shen, L.J. Jacobs, Characterization of progressive microcracking in Portland cement mortar using nonlinear ultrasonics, NDT&E International 41 (2008) 112–118.
[6] C. Payan, V. Garnier, J. Moysan, Applying nonlinear resonant ultrasound spectroscopy to improving thermal damage assessment in concrete, Journal of Acoustical Society of America 121 (2007) 125–131.
[7] S. Kodjo, Contribution à la caractérisation des bétons endommagés par des méthodes de l'acoustique non linéaire. Application à la Réaction alcalis-silice. Ph.D These (in French), Université de Sherbrooke Qc, Canada & Université de Cergy Pontoise, France 2008, p. 140.
[8] K.A. Van Den Abeele, A. Sutin, J. Carmeliet, P.A. Johnson, Micro-damage diagnostics using nonlinear elastic wave spectroscopy, NDT&E International 34 (2001) 239–248.
[9] K. Warnemuende, H.C. Wu, Actively modulated acoustic nondestructive evaluation of concrete, Cement and Concrete Research 34 (2003) 563–570.
[10] J. Chen, A.R. Jayapalan, J.-Y. Kim, K.E. Kurtis, L.J. Jacobs, Nonlinear wave modulation spectroscopy method for ultra-accelerated alkali-silica reaction assessment, ACI Materials Journal 106 (2009) 340–348.
[11] J. Chen, A.R. Jayapalan, J.-Y. Kim, K.E. Kurtis, L.J. Jacobs, Rapid evaluation of alkali–silica reactivity of aggregates using a nonlinear resonance spectroscopy technique, Cement and Concrete Research (2010), doi:10.1016/j.cemconres.2010.01.003.
[12] P. Rasolofosaon, B. Zinszner, P.A. Johnson, Propagation des ondes élastiques dans les matériaux non linéaires, Revue de l'Institut Française du Pétrole 52 (1997) 585–608.
[13] A.R. Guyer, K.R. McCall, K.E.A. Van Den Abeele, Slow elastic dynamics in a resonant bar of rock, Geophysical Research Letters 25 (1998) 1585–1588.
[14] J.A. TenCate, E. Smith, R.A. Guyer, Universal slow dynamics in granular solids, Physical Review Letters 85 (2000) 1020–1025.
[15] J.A. TenCate, Smith Eric, L.W. Byers, Thomas J. Shankland, Slow dynamics experiments in solids with nonlinear mesoscopic elasticity, CP524, Nonlinear acoustics at the turn of the millennium: ISNA 15 edited by W. Lauterborn and T. Kurz, American Institute of Physics, 2000,, 1-56396-945-9 303.
[16] A.R. Guyer, P.A. Johnson, Hysteresis, energy landscapes and slow dynamics: a survey of the elastic properties of rocks, Journal of materials Processing and Manufacturing Science 9 (2000) 14–25.
[17] P.A. Johnson, A. Sutin, J.A. TenCate, Proceedings of the World Congress on Ultrasonics, Paris, France, 2003, pp. 129–132.
[18] P.A. Johnson, P.N.J. Rasolofosaon, Manifestation of nonlinear elasticity in rock: convincing evidence over large frequency and strain intervals from laboratory studies, Nonlinear Processes in Geophysics 3 (1996) 77–88.
[19] Z. Zhu, M.S. Roos, W.N. Cobb, K. Jensen, Determination of the acoustic nonlinearity parameter B/A from phase measurements, Journal of Acoustical Society of America 74 (1983) 1699–1705.
[20] M.A. Breazeale, Finite- amplitude waves in solids, in: M.J. Crocker (Ed.), Handbook of Acoustics, John Wiley and Sons, USA, 1998, pp. 203–210, ISBN 0-471-25293-X.
[21] R.A. Guyer, P.A. Johnson, Nonlinear Mesoscopic Elasticity: The Complex Behavior of Granular Media including Rock and Soil, WILEY-VCH, 2009.
[22] P. Delsanto, M. Scalerandi, Modeling nonclassical nonlinearity, conditioning, and slow dynamics effects in mesoscopic elastic materials, Physical Review 68 (2003) 0641071–0641079.
[23] K.R. Mc Call, R.A. Guyer, Equation of state and wave propagation in hysteretic non linear elastic material, Geophysical Research Letters 99 (1994) 887–897.
[24] E. Barbieri, M. Meo, U. Polimeno, Nonlinear wave propagation in damaged hysteretic materials using a frequency domain-based PM space formulation, International Journal of Solids and Structures 46 (2009) 165–180.
[25] M. Qaisar, Attenuation properties of viscoelastic material, PAGEOPH 131 (4) (1989) 703–713.
[26] N.E. Marcovich, M.A. Villar, Thermal and mechanical characterisation of linear low density poly(etylene)–woodfloor composites, Journal of Applied Polymer Science 90 (2003) 2775–2784.
[27] B.A. Acha, M.M. Roboredo, Norma E. Marcovich, Creep and dynamic mechanical behavior of PP-jute composites: effect of the interfacial adhesion, ScienceDirect Composites: Part A 38 (2007) 1507–1516.
[28] L.H. Sperling, Introduction to Physical Polymer Science, Wiley, New York, 1986, (chapter 8, p. 367).
[29] S.L. Rosen, Fundamental Principles of Polymeric Materials, 2nd ed, Wiley, New York, 1993, p. 299.
[30] K.S. Fancey, A mechanical model for creep, recovery and stress relaxation in polymeric materials, Journal of Materials Science 40 (18) (2005) 4827–4831.
[31] S.A. Husain, R.S. Anderssen, Modelling the relaxation modulus of linear viscoelasticity using Kohlrausch functions, Journal of Non-Newtonian Fluid Mechanics 125 (2005) 159–170.
[32] P. Rivard, G. Ballivy, C. Gravel, F. Saint-Pierre, Monitoring of an hydraulic structure affected by ASR: a case study, Cement and Concrete Research 40 (2010) 676–680.
[33] M. Sargolzahi, A.S. Kodjo, P. Rivard, J. Rhazi, Effectiveness of nondestructive testing for the evaluation of alkali–silica reaction in concrete, Construction and Building Materials 24 (2010) 1398–1403.